Evidence for the formation of quasibound states in an asymmetrical quantum point contact

Phillip M. Wu, Peng Li, Hao Zhang, and A. M. Chang

Phys. Rev. B **85**, 085305 — Published 10 February 2012

DOI: 10.1103/PhysRevB.85.085305

Evidence for the Formation of Quasi-Bound-States in an Asymmetrical Quantum Point Contact

Phillip M. Wu*,[1] Peng Li,[1] Hao Zhang,[1] and A. M. Chang[1]

[1]*Duke University, Department of Physics, Physics Building, Science Drive, Durham NC 27708*

(Dated: October 11, 2011)

Features below the first conductance plateau in ballistic quantum point contacts (QPCs) are often ascribed to electron interaction and spin effects within the single mode limit. In QPCs with a highly asymmetric geometry, we observe sharp resonance peaks when the point contacts are gated to the single mode regime, and surprisingly, under certain gating conditions, a complete destruction of the $2 * e^2/h$, first quantum plateau. The temperature evolution of the resonances suggest non-Fermi liquid behavior, while the overall nonlinear characterizations reveal features reminiscent of the 0.7 effect. We attribute these unusual behaviors to the formation of a quasi bound state, which is stabilized by a momentum-mismatch accentuated by asymmetry.

PACS numbers: 73.63.-b,73.63.Nm

I. INTRODUCTION

The conductance of a quantum point contact (QPC), a narrow constriction connecting two regions of an electron gas, is known to be quantized in units of $G_0 = 2e^2/h$[1,2]. This quantization can be understood within a framework of non-interacting electrons, where the electrons are backscattered by the potential created by the walls of the constriction, and the conductance depends only on the transmission coefficient[3]. However, additional features below the first quantized plateau at $0.7 * G_0$ was observed[4] and cannot be explained within the Landauer formalism. This 0.7 structure has instead been attributed to electron interaction and spin effects[5–9]. Several scenarios have been proposed to account for the 0.7 structure, including the formation of a quasi-bound state in the constriction[10,11], or a novel zigzag Wigner crystal[7]. To date, its origin remains controversial.

In this work, we report unusual features in the conductance of QPCs with an unconventional, asymmetric gate geometry. In contrast to the standard geometry, where two symmetrically placed finger gates define the QPC constriction (with no top gate considered), one of the finger gates is replaced by a long wall gate. We find new features, which point to the formation of a quasi-bound state within the QPC constriction: First, sharp resonance peaks are present when the QPCs are gated below G_0. The resonance line shape conforms to the derivative of the Fermi function, but with an effective temperature which exceeds the lattice temperature at low T. The overall behavior strongly suggests non-Fermi liquid behavior—notably, within the first quantum channel where the resonances are most pronounced, the integrated-area under the conductance curve significantly exceeds that expected for a Fermi-liquid. The energy spacing between successive peaks also exhibits anomalous behavior, and stays fixed even as their energy position is shifted toward the next sub-band continuum. Second and surprisingly, in some geometries, a complete destruction of the first quantized plateau at $2e^2/h$ is observed. Such a behavior was completely unexpected, and from a theoretical perspective has only been seen in numerical simulations when a quasi-bound state is introduced[12,13]. Other features bear similarity to symmetric QPCs: Nonlinear characterizations reveal features reminiscent of the 0.7 structure, such as the 0.25 plateau at high DC bias, and point to the possibility of ferromagnetic properties. We attribute these striking behaviors to the formation of a quasi-bound state, stabilized by a momentum-mismatch accentuated by asymmetry[14].

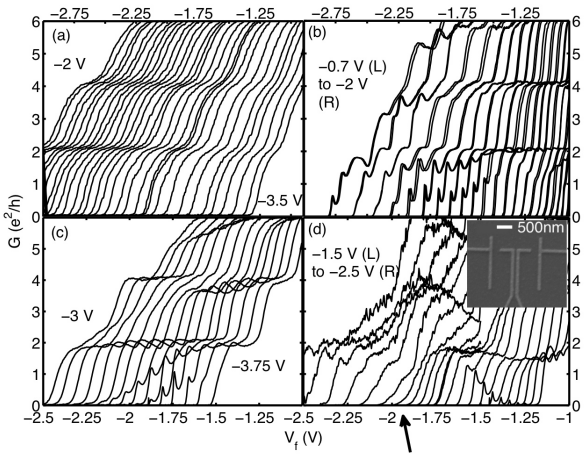

FIG. 1: (a) Unequally gated conductance traces in the symmetric geometry: Each trace is obtained with a fixed voltage on one gate (denoted V_{wall}) while sweeping the voltage on the other gate (V_f). Leftmost trace has V_{wall} =-2 V, which is decremented in 50 mV steps until V_{wall} =-3.5 V in the rightmost trace. (b)-(d) Traces for asymmetric QPCs with lithographic gap widths of (b) 250 nm (c) 450 nm (d) 300 nm, respectively. The temperature is 300 mK for all traces. Doubling of traces in (b) shows reproducibility. Arrow in (d) indicates a trace with fully suppressed $2e^2/h$ plateau. Inset shows two QPCs back to back; one is gated shut during measurement.

II. SAMPLE AND MEASUREMENT

Ti/Au gates were patterned using electron beam lithography on a GaAs/AlGaAs heterostructure containing a 2-dimensional electron gas 80 nm below the surface, with carrier mobility $\mu = 9 \times 10^5$ cm^2/Vs and density $n_{2D} = 3.8 \times 10^{11}$ cm^{-2}. Voltages were applied unequally to the QPC gates by fixing one while sweeping the other. Conductance traces were obtained by applying an excitation voltage of $V_{AC} = 10\mu$V ($< k_BT/e$, where k_B is the Boltzmann constant) across the QPC at 17.3 Hz, and measuring the current using a lock-in amplifier after conversion to a voltage in an Ithaco 1211 current amplifier.

III. NOVEL FEAUTRES IN THE ASYMMETRIC GEOMETRY

In Fig. 1, we contrast the behavior in a standard geometry with symmetric gates (panel (a)) with those in the asymmetric geometry of differing gaps (panels (b)-(d)). In the symmetric case, one finger gate (labeled V_{wall}) is held fixed, while the other (labeled V_f) is swept. The unequal voltage gating shifts the conductance plateaus as V_{wall} is stepped. Typical of several devices made, the 0.7 structure is observable in several traces between V_f = -2.5 V to -1.5 V; no other anomaly is found regardless of the gap width[15]. When the fixed V_{wall} voltage is more negative (left to right), the confinement potential across the gap is expected to become sharper as the total number of quantized plateaus observed decreases[16]. At the same time, the pinchoff voltage where the conductance is shut to zero shifts rightwards, while the density in the single channel (mode) limit decreases.

The behaviors in the asymmetric devices are notably different as shown in Figs. 1(b)-(d). Numerous features are present below and above G_0; here, we focus on the single channel (mode) limit. In particular, sharp resonances below G_0 are observed for all QPC gaps, and in 300 nm gap samples, a completely suppressed G_0 trace is observed. These conductance features are fully reproducible within the same cool-down, as shown in (b). For a given device, different cool-downs from room temperature also give qualitatively similar behavior, despite shifts in position, see Fig. 2. These shifts arise due to the fact that in devices fabricated on modulation-doped GaAs/AlGaAs crystals, the donors which give up the electrons to the 2-d electron gas invariably freeze into different configurations for different cool-downs. Thus the exact shape of the potential landscape in the QPC varies slightly between cool-downs. To further underscore the robustness of our findings, in Fig. 3, we show similar behaviors in yet another 300 nm gap device.

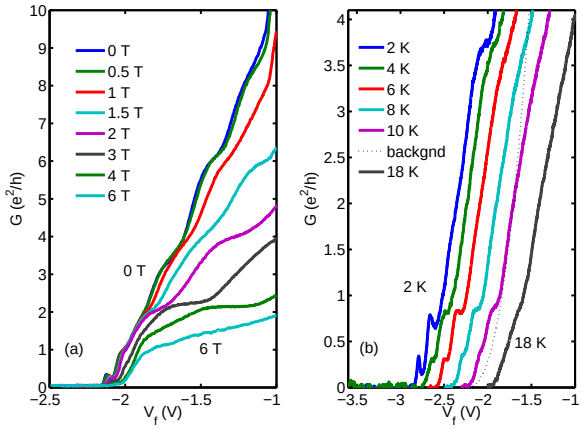

FIG. 2: (a) Evolution of the suppressed $2e^2/h$ plateau in an increasing external magnetic field applied perpendicular to the 2DEG plane at 4.2 K. The $2e^2/h$ plateau recovers around or below 1 T, suggesting an energy of $0.43-0.85meV$ ($5 \sim 10$ K) (taking the value at mid-gap for the Landau gap of 1.7 meV at 1 T). (b) Temperature dependence of the suppression–traces offset horizontally for clarity. The $4e^2/h$ plateau is thermally smeared by 6 K, but the resonance features near e^2/h and $(0.5)e^2/h$ persist up to 10 K, consistent with the energy-scale set by the field dependence. Even at 18 K, an inflection in the conductance at e^2/h is still discernible. Dashed line shows the subtracted background for Fig. 10(a). Note that the slope just above the resonance features appears to be independent of temperature for traces between 2 K - 10 K. (a) and (b) are separate measurements taken from the same device in two distinct cryogenic systems.

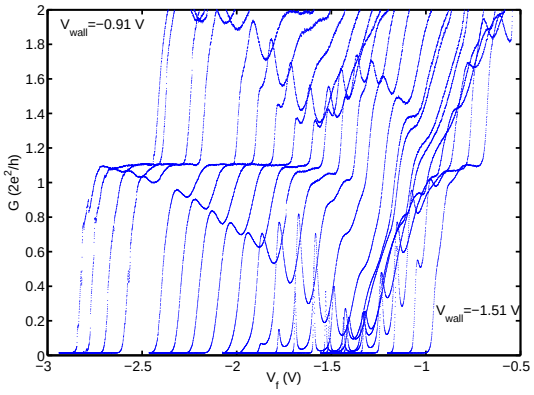

FIG. 3: 300 nm gap sample with 100 nm finger. Traces measured at 300 mK.

A. Resonances and a Simple 1-Dimensional Model of Multiple-Reflection

Resonances in the conductance have been observed previously[17–19], but as we discuss below, the mechanism causing the resonances in our case is completely distinct from previous work. We emphasize that the resonances

arise from geometry, rather than from an impurity residing within, to the side, or underneath the channel. Oscillations on the G_0 plateau were attributed to multiple reflections off the QPC entrance and exit[20]. However, no sharp resonances below G_0 were observed in their case. In our situation, the asymmetric geometry can produce resonances when multiple reflections from the QPC entrance and exit become accentuated due to a momentum-mismatch to the wide 2-d regions[14], in analogy to the strictly 1-d case of a free particle impinging on a rectangular up-step in the potential, see Fig. 4. As the energy of the incoming particle increases, successive resonances are produced as the energy matches and crosses those of quasi-bound states. In the simplest scenario, the occurrence of the bounded states are analogous to resonances in a Fabry-Perot optical interferometer, and corresponds to fitting a half-integer number of wavelengths (on the step), within the length of the step. Because the left and right steps are symmetrical, at a resonance, the transmission is perfect, and attains a value of unity. For completeness, we reproduce the expression for the transmission probability, T, the modulus squared of the transmission coefficient (spin not included):

$$T(E) = \frac{4k^2k'^2}{4k^2k'^2cos^2(k'b) + (k^2 + k'^2)^2sin^2(k'b)} \qquad (1)$$

Here, E is the energy of the particle in the free region outside of the up-step potential, $k = \sqrt{2m^*E}/\hbar$, V_o is the up-step potential value, m^* is the effective mass, and $k' = \sqrt{2m^*(E - V_o)}/\hbar$ the wave number on the step.

In our experiment, there is no reason to expect the lithography to be so ideal as to give rise to a perfectly symmetrical step in its rise and fall. To account for a difference in the coupling at the entrance and at the exit of the QPC, we introduce additional thin regions at the rise and fall of the potential step, where the barriers are not identical (either differing in barrier height, or in thickness, or both, see Fig. 4(b)). This simple model without the inclusion of electron-electron Coulomb interaction, is able to produce traces, as a function of incident electron energy, which qualitatively resembles our data, Fig. 4(c).

Our simple model is further supported by results from a longer channel device, see Fig. 5. Up to five resonance features are visible instead of two. This indicates that the number of resonances increases as the channel length increases, as one would expect from the geometry. The similar behavior observed for all asymmetric devices under multiple thermal cycles suggest that the asymmetric constriction geometry gives rise to the resonances, and this distinguishes our results from those that arise from accidental hydrogenic impurities[17] or from the presence of an intentional side channel in parallel with the QPC[18,19]. Lastly, to make even closer contact with the theoretical literature which analyzed conductance through a QPC, it is worthwhile to point out that early on, several groups, including Szafer and Stone[21], van der Marel and Haanappel[22], Kirczenow[23], Bagwell[24], and others, had analyzed more realistic models with a

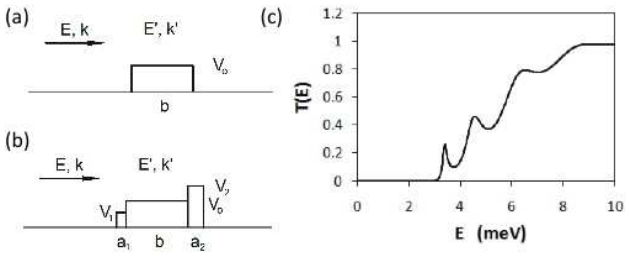

FIG. 4: Drawings of the 1-d model with an up step in the potential showing (a) symmetric rise and fall, (b) unequal rise and fall. (c) Simulated $T(E) = (h/e^2)G$ as a function of incident energy for the model of (b).

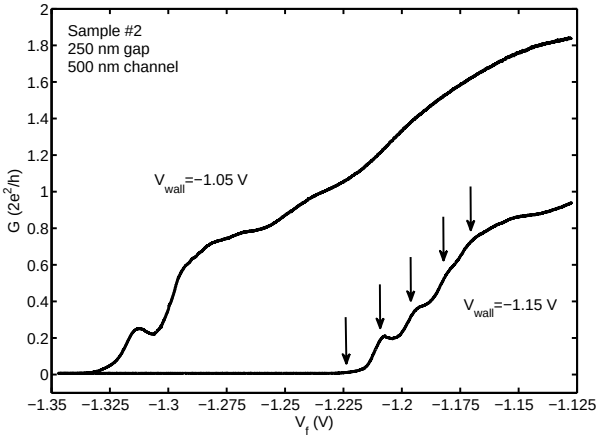

FIG. 5: 250 nm gap, 500 nm long device showing up to 5 resonant features at 4.2 K.

2-d region coupled to a 1-d channel, and with varying degree of abruptness in the transition between the two regions. There, they found that when the transition is abrupt, many resonance-like oscillations are produced. In these analyses, typically the entrance and exit have identical transition regions. Thus at $T = 0$, the transmission becomes unity on resonance. Otherwise, the similarity with the behavior found in our simple model is quite substantial. On the experimental front, Lindelof and Aagesen also reported interference type oscillations on the plateau[20]. They ascribed these to multiple-reflections. However, sharp resonances were not observed.

B. Unusual Characteristics of Resonance Peaks–Peak Width

The resonances we observed exhibit unusual characteristics. One unusual characteristic of the resonance peaks is the apparent constancy of the peak width, even as the peak moves upward on the rising background. The width is estimated using two methods. In the first method, the full-width-at-half-maximum (FWHM) is estimated

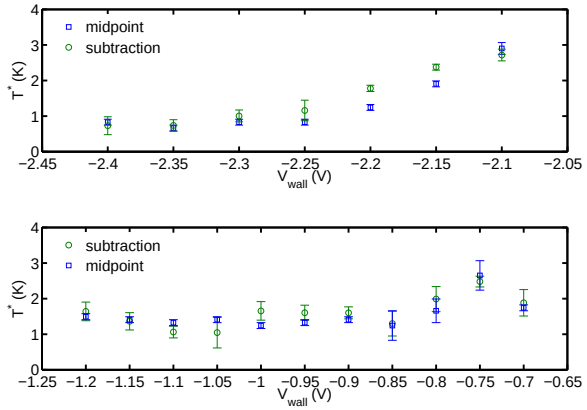

FIG. 6: The effective temperature width, T^*, for the peak in the 300 nm gap QPC in Fig. 3(a) of the main manuscript (top), and for the left peak in the 250 nm gap QPC in Fig. 3(c) (bottom). The results from the two different methods of extracting the width are plotted for comparison.

by taking the difference between the positions to each side of the peak conductance, where the conductance takes on 1/2 the amplitude between the peak and respective trough values. An alternative method is based on first subtracting a background, and then fitting to the derivative of the Fermi-Dirac function: $G = (e^2/h) * \Gamma * (\pi/(4k_BT^*)) * (cosh(\alpha * (V_f - V_{pk})/(2k_BT^*)))^{-2}$. Here α is the lever-arm parameter, V_{pk} the voltage at a resonance peak, and Γ is the intrinsic width of the resonance. The precise form of the background is difficult to determine. A similar difficulties arises in our 1-d model shown in Fig. 4. In this situation, we initially attempted a somewhat arbitrary background in the form $constant * ((V_f - V_p)/x)^y$, with V_p the pinchoff voltage, but later found that using a linear background did not appreciably change the extracted value of the width.

The lever-arm α, which relates V_f measured from pinch-off to an energy, is estimated from magnetic subband depopulation in a perpendicular magnetic field[25–27]. For example, at a typical setting of $V_{wall} \sim -1.6V$ in Fig. 2(a), we find the Fermi energy E_F to be approximately linear in V_f. At the center of the first conductance plateau, E_F has a value $5 - 7$ meV, depending on whether a harmonic oscillator or a square well is used to model the lateral confinement potential. This value is expected to increase as the confinement becomes sharper. For the 300 nm gap device, using the lower bound of $E_F \sim 5$ meV and the difference $\Delta V_f \approx 200$ mV between threshold and the center of the conductance plateau, we find a value of $\alpha = 1/40e$, while at the high end of $7mV$, $\alpha \sim 1/60e$.

The two methods for extracting width yielded similar values when scaled by a constant, see Fig. 6, and when translated into an effective temperature T^*, the widths ($T^* > 700mK$) exceed the ambient temperature, indicating that the peaks are lifetime broadened. For the 1/2 amplitude method, the effective temperature is obtained by dividing the width by $3.5k_B$. In Figure 7 we show expanded views of the resonances and their respective FWHM deduced using the first method for the 300 nm and 250 nm gap devices shown in Fig. 1. In Fig. 7(b), the FWHW is found to be nearly constant over the range -2.45 V$\leq V_{wall} \leq -2.25$ V. On the other hand, the background conductance at the peak position has increased by a factor of ~ 5. A similar trend is found for a double-peak in the 250 nm gap device (Fig. 7 (c) and (d)). In a Fermi liquid, the background conductance is roughly proportional to the inverse life time of the resonance, as is the width. They may be expected to scale together. In our devices, this scaling is grossly violated, indicating unconventional behavior.

C. Unusual Characteristics of Resonances Peaks–Peak Spacing

A second unusual signature is found in the energy spacing between resonances, measured in the difference in their V_f positions, ΔV_f. The simplest interpretation of a double resonance is that the quasi-bound state size is relatively large, allowing two energy levels to exist below the second subband continuum. In Fig. 7(d), we show the energy spacing ΔV_f for the 250 nm gap device of Fig. 1(b). Surprisingly, the spacing is independent of V_{wall} to roughly $\pm 10\%$. The position of the double-peak relative to pinchoff V_f varies monotonically as V_{wall} is varied. Thus the energy position shifts correspondingly. For a Fermi liquid, this spacing tends to decrease as the states come closer in energy position to the continuum (second subband). Here, this does not occur, and the spacing is nearly constant. This highly unexpected behavior is found in all devices exhibiting a double-peak, including those of Fig. 1(b) and (c), and three additional devices as well. This type of relative constant spacing is typically more associated with Coulomb blockade, although, there, one may expect larger variations in the spacing approaching full transmission in the first channel.

D. Temperature Evolution–Evidence for Non-Fermi-Liquid Behavior

A third indication of unusual behavior is found in the temperature evolution of the single-channel regime, where the resonances reside. To analyze the behavior, we divide each trace into two regions in V_f, the first within the first channel, from threshold ($\sim -2.9V$) to $-2.5V$ (where $G \sim 1 * e^2/h$), and the second between $-2.5V$ to $-1.0V$ (where $G \sim 9 * e^2/h$). Below a conductance value of $1 * e^2/h$, the temperature evolution of the conductance traces presented in Fig. 2(b) show strong deviation from the expected behavior of a Fermi-liquid. This deviation

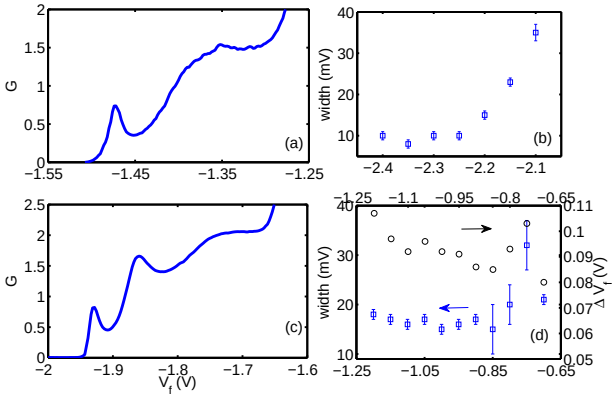

FIG. 7: (a) Expanded conductance versus V_f plot for asymmetric geometry with 300 nm gap, at V_{wall} =-2.25 V, showing a resonance peak. (b) The full-width-at-half-maximum (FWHM) as a function of V_{wall}. (c) Expanded plot for asymmetric geometry with 250 nm gap, at V_{wall} =-1 V. (d) FWHM for the left peak and double-peak spacing ΔV_f as a function of V_{wall}. The FWHM for right peak exhibits a similar trend. The temperature is 300 mK.

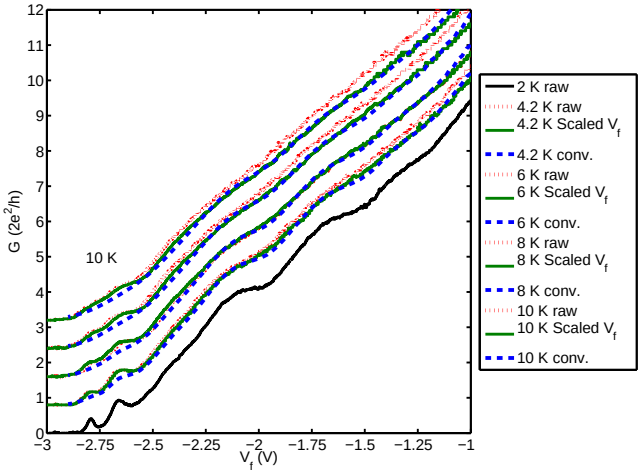

FIG. 8: The conductance trace for the second 300 nm gap QPC device. Raw data is from Fig. 2(b) (shown as thin dashed lines here). Raw data plotted versus rescaled V_f to account for changes in the gating due to a temperature rise (solid lines). The simulated Fermi-liquid behavior, obtained by the convolution of Eq. 2 is also shown (thick dotted lines). Note that below $G \sim 1{*}e^2/h$, the simulation fails to reproduce the data, and falls below it.

is significant when compared to the agreement achieved in the region above $1 * e^2/h$, up to an upper cut-off of $\sim 9{*}e^2/h$. In this upper region, the Fermi-liquid scenario works extremely well, to $\sim 1\%$ accuracy.

To be more precise, the division of the lower and upper regions should be placed at $G \sim 2e^2/h$, where the first channel resides. In fact, in Fig. 8 below, we will show that deviation from Fermi-liquid behavior is present up to this point. Here, we wish to highlight the region containing the resonances close to threshold. Thus, we set the division at $1 * e^2/h$ instead.

We place our focus in the temperature range $2-10K$, as above $10K$, the resonances peaks become difficult to resolve due to excessive thermal smearing. It then becomes difficult to determine the threshold of conduction with sufficient precision; often the threshold can shift at higher temperatures due to residual rearrangement in the configuration of donor dopants. When the resonances are clearly visible, the positions of the resonances provide reliable reference points in order to line up traces at different temperatures.

Aside from such shifts in the threshold, differences in gating characteristics invariably occurs as the temperature rises. As an example, the positions where $G = 4{*}e^2/h$ and $G = 6{*}e^2/h$ in the center of the second and third quantized plateaus, respectively, are expected to be temperature invariant. However, experimentally, this invariance is rarely seen, as a result of the slight rearrangement of dopant configuration. To account for this effect, we first utilize the positions of the resonances to account for any shift, followed by a rescaling of the V_f values to match the positions of the $G = 4 * e^2/h$ and $G = 6 * e^2/h$ plateau centers at all temperatures. The ideal value of the scale factor is of course 1 (unity). We find that at $10K$, which gives the largest scale factor, a scale factor of 1.05 is required.

In Fig. 8, we present the raw data for T between $2-10K$ in thin dashed lines, and the shifted/scaled data in solid lines. Successive temperatures are offset for clarity. To test the validity of the Fermi-liquid picture in each region, below $1 * e^2/h$ for the lower and above $1 * e^2/h$ up to $9 * e^2/h$ for the upper region, we generate a series of theoretical curves for each temperature, shown as thick dotted lines. For a Fermi liquid, the conductance at a finite temperature is given by the convolution of the derivative of the Fermi-Dirac function, with the transmission probability:

$$G = I/V = \frac{e^2}{h}\int_{-\infty}^{\infty}[\frac{\partial f(E-E',kT)}{\partial E'}]T(E')dE', \quad (2)$$

where $T(E')$ is the transmission probability at energy E' at $T = 0$. For our calculations, we take $G(\alpha{*}(V_f - V_{th})) = I(E)/V$, which relates the measured quantities in terms of the finger gate V_f to an energy, where α is the lever arm.

If we take $E' = E_1$, $T(E_1)$ represents the transmission probability for incident energy E_1 at zero temperature. Ideally, $T(E_1) = (h/e^2)G(E_1, T = 0)$. However, our data set has a lowest temperature of $T = 2K$. We thus approximate $T(E_1)$ by $T(E_1) \approx (h/e^2)G(E_1, T = 2K)$. To achieve consistency of the widths for both peaks relative to the temperature, we set E_F at the high end with $E_F = 7meV$, rather than $5meV$, yielding a value for α of $\alpha = 7meV/450mV = 0.0156e \approx 1/65e$. Based on

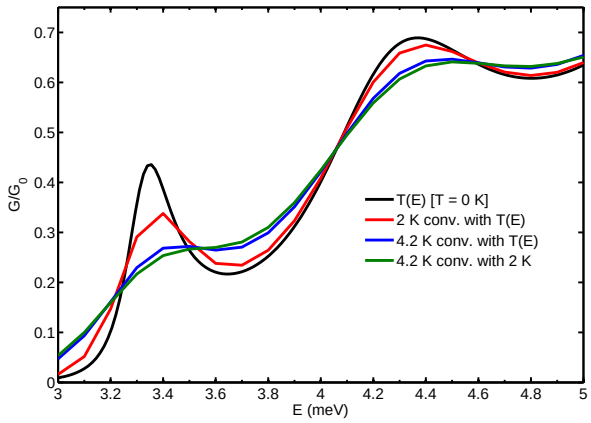

FIG. 9: Convolution of the simulated $T(E_1) = (h/e^2)G$ based on the model of Fig. 4(b) (spin not included), with the derivative of the Fermi-Dirac function, to gauge the error introduced by approximating the $T(E_1)$ value (for $T = 0$) (yellow), with that deduced from the $G(E_1)$ conductance trace at $T = 2K$ (blue). At $T = 4.2K$, the convolution with the approximate $T(E_1)$ (red) shows minimum deviation from the convolution with the $T = 0$ $T(E_1)$ (black).

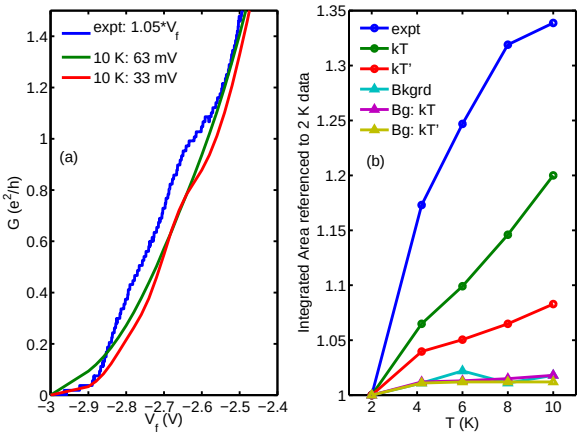

FIG. 10: (a) Conductance trace of Fig. 2 for T = 10 K, below $G \sim 1 * e^2/h$ (blue). The Fermi-liquid temperature convolution using Eq. (1), based on kT being equivalent to 63 mV (green). To reproduce the broadened resonances seen in the data, it was necessary to reduce the correspondence to an unphysical kT' value of 33 meV (red). (b) The integrated areas contrasting the agreement of the Fermi-liquid convolution with data in the upper (background) region, where $1 * e^2/h \leq G \leq 9 * e^2/h$ (bottom 3 curves), versus the striking disagreement within the lower region for $G < 1 * e^2/h$.

these values, the left peak in the $2K$ trace is thermally-broadened, while the right peak, at roughly twice the width, is life-time broadened.

Since all other temperatures are at least a factor of two higher than $2K$, with the next lowest at $4.2K$, one may suspect that this approximation of using the $T = 2K$ curve to approximate the $T = 0$ transmission may be adequate. To demonstrate this, we perform a comparison with the simulated trace shown in Fig. 4(c), for the 1-d "rectangular" up-step model. In Fig. 9, the solid line represents the simulated zero temperature value for $T(E_1)$. A convolution using Eq. 2 is performed at $T = 4.2K$ to produce the dotted curve. Next, a convolution at $T = 2K$ produces an approximate $T(E_1)$, which in turn is used in a convolution at $4.2K$, to yield the dashed curve. It is clear that the difference between the two curves (dotted and dashed) is minimal, and appears to be comparable to or less than the noise in the data of Fig. 8.

It is apparent in Fig. 8 that in the upper region beyond $1 * e^2/h$, the convolution reproduces the data with a high degree of accuracy, while in the lower region, the convolution falls significantly below the data. Notably, the convolution fails to capture the qualitative behavior in the lower region as can be seen in Fig. 10(a), which plots the results of the convolution compared with data for $T = 10K$. The featureless simulated curve corresponds to a conversion of kT to a V_f, $10K : kT \rightarrow 63mV$, which is based on our best estimate for the Fermi-energy ($E_F \approx 7meV$) at the position of the first channel, at which the center of the $1 * 2e^2/h$ normally resides. This trace falls below the experimental curve and is completely devoid of any hint of the resonances due to excessive thermal smearing. To simulate the broadened peaks visible in the data, it was necessary to reduce the correspondence to $kT' \rightarrow 33mV$, an unphysical value, yielding the second convolution trace. In this case, the overall trace falls even lower.

To characterize these simulated traces and compare to experiment, we calculated the integrated area underneath each conductance curve for the lower and upper regions referenced to the $2K$ value, Fig. 10(b). It is striking that in the upper region where one expects the Fermi-liquid picture to be valid, agreement between data and the convolution curves at the $\sim 1\%$ level is readily achieved. In stark contrast, for the lower region below $1 * e^2/h$, a substantial discrepancy, in excess of 10% is found, well in excess of noise. This provides clear evidence that the Fermi-liquid description is no longer adequate. This enhanced integrated area is a signature of a 1-d Luttinger liquid, in which interaction modifies the temperature evolution of the conductance, leading to an enhancement. In a sense, this is a remarkable result. Our channel length is short, with a lithographic length of 100 nm. Accounting for a depletion distance from the gating, the channel will not exceed 300 nm in length, and only 5 - 8 electrons will reside in the single-mode channel. Normally, when a short Luttinger liquid is strongly coupled to 2-d leads, the signature of the Luttinger liquid correlation is difficult to observe, as the long wave-length characteristics is cut-off by the finite size. Here, with the presence of the resonances, which are coupled with intermediate strength to the channel, we have uncovered clear indications of non-Fermi-liquid behavior.

IV. ABSENCE OF THE $2e^2/h$ FIRST QUANTIZED CONDUCTANCE PLATEAU

Aside from the resonances, surprisingly, for the 300 nm gap, the $2e^2/h$ plateau is completely absent under certain gating conditions. In Fig. 1(d), the arrow indicates the trace, for which this first plateaus has been fully suppressed. Starting from threshold in the conductance, the trace rises directly toward a plateau close to but below $4e^2/h$ in value, without any hint of a $2e^2/h$ plateau. A similar behavior is found for a second 300 nm gap device, as can be seen in Fig. 2, as well as for a third device in Fig. 3. This suppression is also seen in a 250 nm gap device, while the general weakening of the plateau (less flat) is observed in all devices. For some devices, this weakening occurs quasi-periodically in V_{wall} settings. Because the V_f values adjust to V_{wall}, the effective channel length is correspondingly modulated due to carrier depletion adjacent to the V_f gate.

This suppression is associated with a sizable energy scale. One estimate of the energy scale is obtained by applying a magnetic field B_z perpendicular to the 2DEG plane, as shown in Fig. 2(a). No change is observed up to 0.5 T, which provides a lower bound estimate of $\sim 0.43meV$ ($\sim 5K$) (taking the value at half the Landau gap). At 1 T, an inflection near $2e^2/h$ is noticeable, suggesting an upper bound of 10 K. This is a rather large energy scale. Beyond 3 T, the system enters the filling factor $\nu = 2$ quantum Hall regime (only the ground subband remains), and a $2e^2/h$ plateau is clearly visible, which indicates that the cyclotron confinement has exceeded the suppression scale. The suppression of double peak features near $0.5 * e^2/h$ and e^2/h in a magnetic field suggests that these are not resonances associated with localized impurities, as they would strengthen at stronger confinement in an applied B_z. Instead, their suppression is in accord with a multiple-reflection scenario. At stronger fields, signature of the Zeeman spin gap at e^2/h re-develops. In a magnetic field applied *parallel* to the the 2DEG of up to $6T$ (data not shown), no change is observed, suggesting the spins may already be polarized at zero field.

Temperature dependence of the suppressed $2e^2/h$ plateau is shown in Fig. 2(b). The quantized conductance of the $4e^2/h$ plateau is washed out by thermal averaging above 6 K; however, there still appears to be a clear feature below $\sim e^2/h$, which persists up to 10 K. At 18 K, the features near pinch-off are thermally smeared, but an inflection in the curvature near e^2/h remains. This supports the high energy scale estimate of electron interactions in the conducting channel. Based on our estimate, the $2e^2/h$ plateau should return once the temperature exceeded ∼6-10 K. Unfortunately, that is not observable as above 6 K conductance quantization is already thermally smeared.

The behavior found in our 300 nm devices of a direct jump in conductance from pinchoff to $\sim 4e^2/h$ has been suggested to be related to formation of incipient lattice in the case of a symmetric QPC[28–30]. Alternatively, numerical simulations have shown such features to be possible when considering a quantum dot embedded in the 1D channel, when the dot potential is attractive and gives rise to a quasi-bound state[12,13]. Importantly, the dot potential contained a repulsive boundary region. One possible cause of the suppression may be that the effective potential seen in the first channel possesses a sufficiently high barrier, arising from this repulsive boundary region, which even at the center of the first channel, is able to partially block the transmission[12].

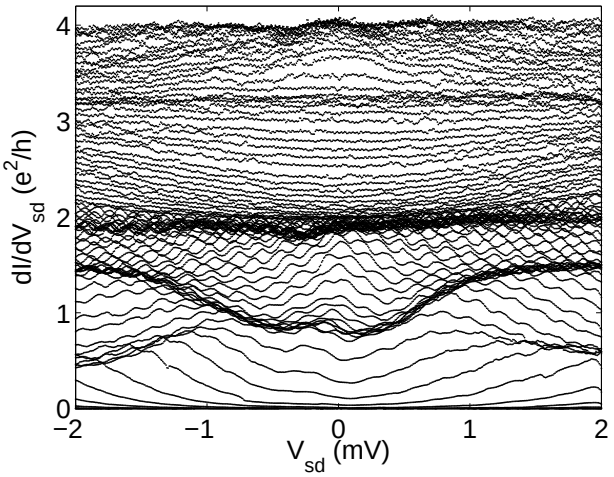

FIG. 11: DC source drain bias dependence (V_{SD}) for the 250 nm gap sample, Fig. 1(b), at zero applied magnetic field and V_{wall} =-1.2 V. Strong bunching at e^2/h and transitions to $1.5e^2/h$ at ∼1 mV are seen. All traces measured at 300 mK in an Oxford He3 refrigerator.

Theoretically stabilization of a quasi-bound state have been proposed to arise from Coulomb interaction[10,11]. Thus, the suppression may also require a high energy scale Coulomb interaction in the QPC bound state, despite a recent theoretical calculation suggesting that momentum-mismatch alone is sufficient to give rise to a quasi-bound state[14]. The presence of multiple-reflections could lead to a build-up of carrier density in different positions. When under the right conditions, this build-up may appear at an end of the QPC, causing a repulsive bump within a self-consistent picture. Whereas in symmetric QPCs the existence of a quasi-bound-state is strongly debated[10,30], and detailed studies appears to rule out their presence, in the asymmetric QPCs studied here, the momentum-mismatch could be accentuated, and in conjunction with Coulomb interaction, accentuated multiple-reflections may render a quasi-bound-state more likely to occur.

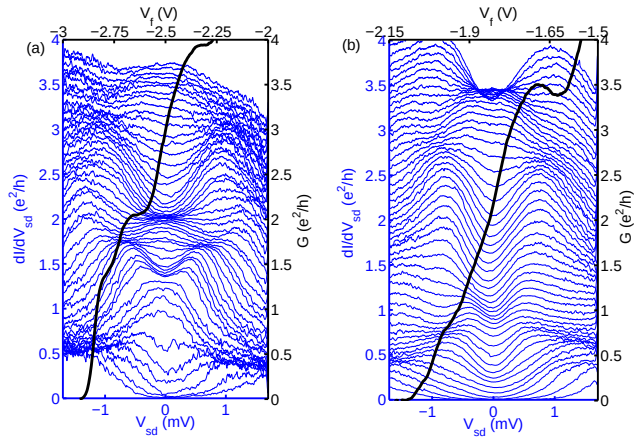

FIG. 12: Differential conductance versus DC source-drain bias, V_{SD}.(a) Traces where strong feature at $1.5e^2/h$ exists in the conductance (black) are shown along with the corresponding response under DC bias (blue). (b) A DC bias trace (blue) with a strongly suppressed $2e^2/h$ (conductance versus gate in black). All traces are taken at 4.2 K.

V. NON-LINEAR DIFFERENTIAL CONDUCTANCE DI/DV

In Fig. 11, the differential conductance versus DC source-drain bias at 300 mK is presented, obtained by adding an AC bias to the DC bias and measuring the AC signal in a lock-in amplifier. The bunching of the traces in the differential conductance versus DC bias corresponds to quantization plateaus in the nonlinear differential conductance. Note that an e^2/h plateau typically develops under a strong magnetic field which spin polarizes the electrons. Here, no magnetic field is applied. At a high DC bias around 1 mV, the e^2/h bunch evolves to $1.5e^2/h$, which is reminiscent of the 0.7 effect[4]. Based on this voltage, we estimate the spin splitting to correspond to an applied field of nearly 40 T.[6] Formation of a ground state magnetic moment is often surmised in light of the strong electron interaction effects in our QPC[9]. More specifically, Hund rule coupling of the electrons strongly bounded to the QPC can give rise to the magnetic moment[14]. Although the detailed magnetic behavior and additional ripples in the differential conductance remain to be understood, these traces provide further evidence for the formation of a quasi-bound state in the QPC.

In Fig. 12, the differential conductance dI/dV versus DC source-drain bias taken at 4.2 K is shown for several asymmetric gate settings: (a) where a $1.5 * e^2/h$ (or 0.7 effect) feature is clearly visible at $V_{wall} = -1.5$V and (b) conductance with the $2*e^2/h$ plateau completely suppressed to e^2/h, taken during a separate cooldown. There is a weak plateau at e^2/h even at zero DC bias in (B), but there is no $2 * e^2/h$ plateau as in (a). In contrast to the peak structure in (a) from $1.5 - 2 * e^2/h$, the differential conductance in (b) is strongly suppressed throughout. This is in contrast to[6], where zero bias peaks exist below e^2/h and are suppressed under a parallel magnetic field of 7 T. The suppression observed here is another possible indication of spin polarization. At higher bias, plateaus at $0.5 * e^2/h$ develop in both panels.

VI. CONCLUSION

In conclusion, we present evidence for the formation of quasi-bound states in an asymmetrical QPC. The presence of resonances is unique to our geometry, and provides a direct indication for the existence of quasi-bound states. The quasi-bound state is likely stabilized from an exaggerated momentum-mismatch at the openings of the asymmetric geometry. Second, the unusual suppression of the $2 * e^2/h$ plateau also suggests a bound state[14], and possibly strong interaction effects[28]. Third, we find evidence of electron interaction effects. These are manifest in the temperature evolution of the resonance peaks in the single-channel regime. These unusual features are still far from understood, and their relation with novel correlated states, such as the zigzag Wigner crystal states[7,28] still remains to be investigated.

Acknowledgments

We thank H.U. Baranger, E. Mucciolo, G. Finkelstein, and M.K. Wu for useful discussions, S. Teitsworth for use of his dewar, M. Melloch for crystal and H. Zhang for fabricating and measuring several additional samples. Work supported in part by by NSF DMR-0701948, and the Institute of Physics, Academia Sinica, Taiwan.

*Present Address: Division of Solid State Physics/Nanometer Structure Consortium, Lund University, Box 118, 221 00 Lund, Sweden.

[1] B. J. van Wees, H. van Houten, C. W. J. Beenakker, J. G. Williamson, L. P. Kouwenhoven, D. van der Marel, and C. T. Foxon, Phys. Rev. Lett. **60**, 848 (1988).

[2] D. A. Wharam et al., J. Phys. C: Solid State Phys. **21**, L209 (1988).

[3] R. Landauer, Phil. Mag. **21**, 863 (1970).

[4] K. J. Thomas, J. T. Nicholls, M. Y. Simmons, M. Pepper, D. R. Mace, and D. A. Ritchie, Phys. Rev. Lett. **77**, 135 (1996).

[5] K. J. Thomas, J. T. Nicholls, N. J. Appleyard, M. Y. Simmons, M. Pepper, D. R. Mace, W. R. Tribe, and D. A. Ritchie, Phys. Rev. B **58**, 4846 (1998).

[6] S. M. Cronenwett, H. J. Lynch, D. Goldhaber-Gordon, L. P. Kouwenhoven, C. M. Marcus, K. Hirose, N. S. Wingreen, and V. Umansky, Phys. Rev. Lett. **88**, 226805 (2002).

[7] K. A. Matveev, Phys. Rev. Lett. **92**, 106801 (2004).

[8] D. J. Reilly, Phys. Rev. B **72**, 033309 (2005).

[9] T. Rejec and Y. Meir, Nature **442**, 900 (2006).

[10] Y. Meir, K. Hirose, and N. S. Wingreen, Phys. Rev. Lett. **89**, 196802 (2002).

[11] K. Hirose, Y. Meir, and N. S. Wingreen, Phys. Rev. Lett. **90**, 026804 (2003).

[12] J. H. Bardarson, I. Magnusdottir, G. Gudmundsdottir, C. S. Tang, A. Manolescu, and V. Gudmundsson, Phys. Rev. B **70**, 245308 (2004).

[13] V. Gudmundsson, Y. Y. Lin, C. S. Tang, V. Moldoveanu, J. H. Bardarson, and A. Manolescu, Phys. Rev. B **71**, 235302 (2005).

[14] T. Song and K.-H. Ahn, Phys. Rev. Lett. **106**, 057203 (2011).

[15] F. Wakaya, J. Takahara, S. Takaoka, K. Murase, and K. Gamo, Jpn. J. Appl. Phys. **35**, 1329 (1996).

[16] M. Buttiker, Phys. Rev. B **41**, 7906 (1990).

[17] P. L. McEuen, B. W. Alphenaar, R. G. Wheeler, and R. N. Sacks, Surface Science **229**, 312 (1990).

[18] Y. Yoon, L. Mourokh, T. Morimoto, N. Aoki, Y. Ochiai, J. L. Reno, and J. P. Bird, Phys. Rev. Lett. **99**, 136805 (2007).

[19] Y. Yoon, M. G. Kang, T. Morimoto, L. Mourokh, N. Aoki, J. L. Reno, J. P. Bird, and Y. Ochiai, Phys. Rev. B **79**, 121304 (2009).

[20] P. E. Lindelof and M. Aagesen, J. Phys.: Condens. Matter **20**, 164207 (2008).

[21] A. Szafer and A. D. Stone, Phys. Rev. Lett. **62**, 300 (1989).

[22] D. van der Marel and E. G. Haanappel, Phys. Rev. B **39**, 7811 (1989).

[23] G. Kirczenow, Phys. Rev. B **39**, 10452 (1989).

[24] P. F. Bagwell, Phys. Rev. B **41**, 10354 (1990).

[25] B. J. van Wees L. P. Kouwenhoven, H. van Houten, C. W. J. Beenakker, J. E. Mooij, C. T. Foxon, and J. J. Harris, Phys. Rev. B **38**, 3625 (1988).

[26] D. A. Wharam et al., Phys. Rev. B **39**, 6283 (1989).

[27] J. F. Weisz and K. F. Berggren, Phys. Rev. B **40**, 1325 (1989).

[28] W. K. Hew, K. J. Thomas, M. Pepper, I. Farrer, D. Anderson, G. A. C. Jones, and D. A. Ritchie, Phys. Rev. Lett. **102**, 056804 (2009).

[29] L. W. Smith, W. K. Hew, K. J. Thomas, M. Pepper, I. Farrer, D. Anderson, G. A. C. Jones, and D. A. Ritchie, Phys. Rev. B **80**, 041306(R) (2009).

[30] F. Sfigakis, C. J. B. Ford, M. Pepper, M. Kataoka, D. A. Ritchie, and M. Y. Simmons, Phys. Rev. Lett. **100**, 026807 (2008).